A Unified Single-Event Microkinetic Model for Alkane Hydroconversion in Different Aggregation States on Pt/H−USY-Zeolites

C. S. Laxmi Narasimhan,[†] Joris W. Thybaut,*[,†] Johan A. Martens,[‡] Pierre A. Jacobs,[‡] Joeri F. Denayer,[§] and Guy B. Marin[†]

Laboratorium voor Petrochemische Techniek, Ghent University, Krijgslaan 281 S-5, B-9000 Gent, Belgium, Centrum voor Oppervlakchemie en Katalyse, Katholieke Universiteit Leuven, Kasteelpark Arenberg 23, B-3001 Heverlee, Belgium, and Chemie Ingenieurstechniek, Vrije Universiteit Brussel, Pleinlaan 2, B-1050 Brussel, Belgium

Received: September 2, 2005; In Final Form: January 27, 2006

A single-event microkinetic model for the catalytic hydroconversion of hydrocarbons on Pt/H−US-Y bifunctional zeolite catalysts developed for low-pressure vapor phase conditions was extended to cover high-pressure vapor phase and liquid phase conditions. The effect of the density of the bulk hydrocarbon phase on the physisorption as well as on the protonation steps of the reaction network was accounted for explicitly and can be interpreted in terms of "*compression*" of the hydrocarbon sorbate inside the zeolite pores and "*solvation*" of the catalyst framework by the dense bulk hydrocarbon phase. The bulk phase density effect on the physisorbed state is described via a single excess free enthalpy of physisorption. A dense bulk hydrocarbon phase destabilizes the sorbate molecules inside the catalyst pores. An expression of the excess free enthalpy of physisorption involving the fugacity coefficient and a zeolite dependent factor allows description of physisorption data. Typical excess free enthalpy values are in the range 1.5−5.1 kJ mol^{-1} increasing with carbon number in the series of C_5−C_{16} alkanes. At high-pressure vapor phase and liquid phase conditions, the excess standard protonation enthalpy is estimated at −7.8 kJ mol^{-1} leading to relatively more stable carbenium ions at dense bulk phase conditions. As a result of the excess physisorption and protonation properties, the lightest hydrocarbons in mixtures are more competitive at dense phase conditions and their conversion is enhanced compared to low-density conditions.

Introduction

Hydroconversion on Pt/H−USY-zeolites follows a classical bifunctional reaction mechanism. (De)hydrogenation reactions occur on the metal sites while protonation of the unsaturated components occurs on the acid sites. The protonation is followed by carbenium ion reactions, such as skeletal isomerization and cracking. Physisorption of the molecules precedes the reactions in the zeolite pores.

Denayer et al.[1,2] reported differences in rate coefficients for gas and liquid phase hydroconversion reactions with binary hydrocarbon mixtures. The rate of *n*-heptane conversion relative to *n*-nonane was enhanced by more than a factor of 2 in the liquid phase indicating that *n*-heptane is more competitive with *n*-nonane at the latter conditions. Similar observations were reported for hydroconversion of other mixtures.[3] The competition effects were found to become more pronounced for sorbents exhibiting higher heats of physisorption.[1,2] The effect of the bulk phase density on elementary reactions is well documented.[4] For metal catalysis, the reactant aggregation state is reported to strongly influence the reaction paths and rates.[4−9] Similar considerations can be made for acid catalysis although literature on this subject is scarce.[8]

In the description of vapor phase hydroconversion, data available on each of the elementary steps obtained from independent experiments are preferably used. E.g., physisorption data obtained at vapor phase conditions[10] are used to determine the physisorption equilibrium coefficient while rate parameters are estimated from kinetic data. The same approach is followed in this work for liquid phase kinetics. Reference values are used for physisorption and kinetic parameters. The only adjustable parameters account explicitly for the bulk phase density effect on the physisorption and on the kinetics.

At low pressures, the vapor phase has a low density and can be considered as an ideal gas. Physisorption at these conditions typically falls in the Henry regime.[11,12] The surface enrichment, defined as the density difference between physisorbed phase and the bulk phase, is high[13] and varies with zeolite type and composition. In the Henry regime surface enrichment leads to an increase of the reaction rates. Deviations from the Henry regime occur with increasing bulk phase density and lead to a decrease of the surface enrichment.[12−22] Aranovich and Donohue[20,21] have comprehensively analyzed the effect of bulk phase density on adsorption on solid surfaces and stressed the destabilization of the physisorbed phase at dense bulk phase conditions. The latter was termed as "adsorption compression effect": adsorbates undergo a compression and, hence, start repelling each other resulting in a lowering of the surface enrichment.[20−22] The extent of this interaction varies with the density of the bulk fluid phase. Although this compression effect is studied at surfaces, its application can be extended to a microporous sorbent. Protonation is also affected by the bulk phase density.[4,8] The higher bulk phase density leads to a more pronounced carbenium ion stabilization compared to a low-

* Corresponding author. Tel: +32 9 264 45 19. Fax: +32 9 264 49 99. E-mail: Joris.Thybaut@UGent.be.
[†] Ghent University.
[‡] Katholieke Universiteit Leuven.
[§] Vrije Universiteit Brussel.

10.1021/jp054981j CCC: $33.50
Published on Web 03/10/2006

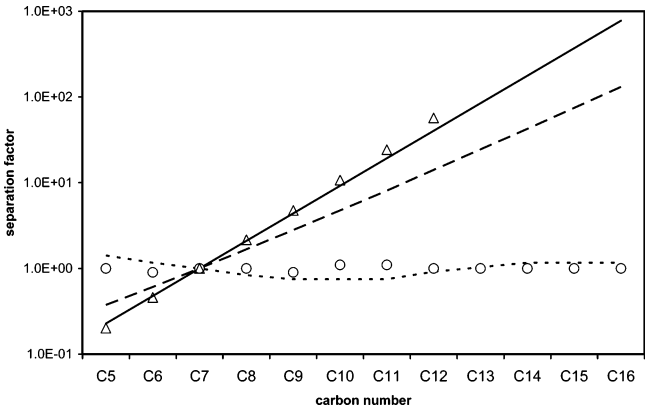

Figure 1. Separation factors, eq 1, at 506 K and 8 MPa as a function of the carbon number. Symbols, experimental vapor phase, △,[10] and liquid phase, ○,[23] data. Lines: vapor phase calculated from eq 20, full line; liquid phase, calculated from eq 21, i.e., only accounting for the bulk phase nonideality, long-dashed line; liquid phase, calculated from eq 19, i.e., accounting for the bulk phase nonideality and the excess behavior in physisorption with $c^E = 1.55$ kJ mol^{-1}, short-dashed line. Vapor phase data have been measured using a $H_2 + C_8 + C_n$ mixture[10] and liquid-phase data using a $C_8 + C_n$ mixture.[23] The data have been recalculated afterward to C_7 as reference component instead of C_8.

density bulk phase.[8] The enhanced stabilization of the carbenium ions leads to higher concentrations and, hence, to higher rates of subsequent carbenium ion reactions, given that the alkene concentrations are equal.

Clearly, the effect of density of the bulk phase on the kinetics needs to be accounted for in a fundamental way to describe liquid phase kinetics. The need is even more significant considering that most industrial hydroconversion units work under liquid phase conditions. In the present work a fundamental interpretation of the effect of the bulk phase density on the various elementary steps in hydroconversion is presented. The effect on physisorption has been investigated and determined based on separate physisorption data. The effect on protonation was assessed using kinetic data.

Procedures

Physisorption Data. The separation factor at every point of a binary physisorption isotherm is defined as

$$\alpha_{i-j} = \frac{y_i/y_j}{x_i/x_j} = \frac{C_{\mathrm{phys},i}/C_{\mathrm{phys},j}}{C_i/C_j} \tag{1}$$

y_i and x_i represent the mole fractions of components i and j in the physisorbed phase and in the bulk fluid phase. At ideal vapor phase conditions the separation factor corresponds to the ratio of the corresponding Henry coefficients

$$\alpha_{i-j} = \frac{H_i}{H_j} \tag{2}$$

Because binary mixtures are concerned, the separation factor can be rewritten as

$$\alpha_{i-j} = \frac{y_i/(1-y_i)}{x_i/(1-x_i)} \tag{3}$$

and, consequently, the composition of the physisorbed phase in equilibrium with the bulk phase can be described as

$$y_i = \frac{\alpha_{i-j}x_i}{(1+\alpha_{i-j}x_i - x_i)} \tag{4}$$

in which α_{i-j} is assumed to be constant over the entire range of fluid phase composition x_i.

Denayer et al.[23] have reported liquid phase physisorption properties in terms of partition coefficients, which are equivalent to separation factors, for C_6-C_{16} *n*-alkanes. Figure 1 shows recalculated experimental values for separation factors with respect to *n*-heptane for both aggregation states. For the vapor phase conditions, the Henry coefficients increase exponentially with the carbon number. This leads to separation factors lower than 1 for alkanes lighter than heptane and higher than 1 for alkanes heavier than heptane at vapor phase conditions. Calculating the Henry coefficients from the linear relationships as proposed by Denayer et al.[10] leads to separation factors which are in good agreement with the experimentally observed values. The observed separation factors at liquid phase conditions are close to 1 and independent of the carbon number, indicating negligible separation among alkanes on USY. Some of the corresponding binary physisorption isotherms are presented in Figure 2a. A strong preferential physisorption of the heavier hydrocarbons is observed at vapor phase conditions. The liquid phase binary physisorption isotherms between *n*-heptane and *n*-octane and *n*-nonane and *n*-decane are presented in Figure 2b. No preferential physisorption behavior occurs. All alkanes have an equal competitiveness resulting in equal mole fractions in the fluid phase as well as in the physisorbed phase.

Kinetic Data. Vapor- and liquid phase *n*-C_7:*n*-C_9 binary mixture hydroconversion have been performed on Pt/CBV-720 and reported elsewhere.[1,2] Vapor phase equimolar *n*-C_7:*n*-C_9 binary mixture hydroconversion was performed in a plug flow reactor at $W/F_{\mathrm{HC},0} = 80-500$ kg s mol^{-1}, $T = 503$ K, $p_t =$

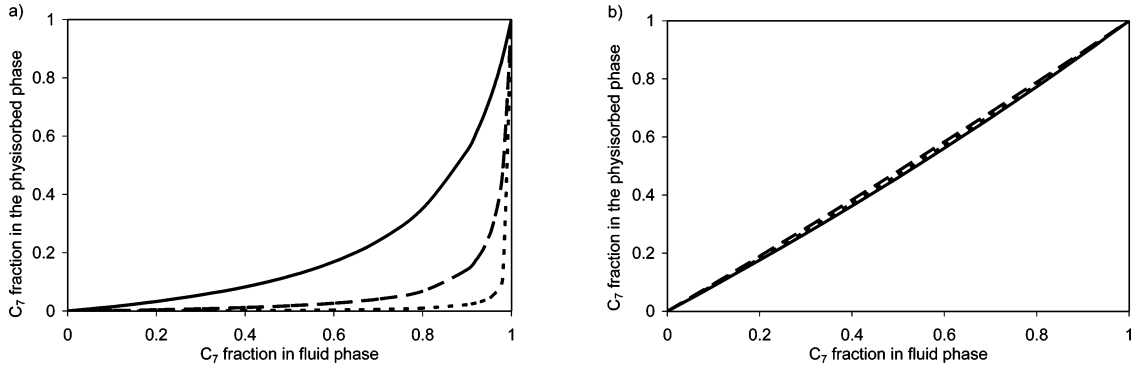

Figure 2. Binary physisorption isotherms constructed from experimental data reported in refs 10 and 23 at ambient conditions for *n*-heptane and *n*-octane (full line), *n*-nonane (long-dashed line), and *n*-decane (short-dashed line) at (a) vapor phase conditions and (b) liquid-phase conditions. Ambient conditions are being used because the difference between vapor and liquid physisorption behavior is most pronounced at these conditions.

0.45 MPa, and H_2/HC molar inlet ratio = 13.1. At these experimental conditions, "ideal" hydroconversion occurs, i.e., (de)hydrogenation reactions are quasi-equilibrated. Liquid phase hydroconversion of an equimolar *n*-C_7:*n*-C_9 mixture was performed in a plug flow reactor at 503 K, 10 MPa, and a molar hydrogen to hydrocarbon inlet ratio of 0.5. The space time ranged from 100 to 500 kg s mol^{-1}.[1,2]

Parameter Estimation. Parameter estimations were performed using the Levenberg−Marquardt method for minimization of the following objective function, $S(b)$, considering the full error variance−covariance matrix calculated from observed and calculated physisorbed mole fractions

$$S(b) = \sum_{q=1}^{n_{ob}} \sum_{i=1}^{n_{resp}} \sum_{j=1}^{n_{resp}} \sigma_{i,j}[y_{i,q} - \hat{y}_{i,q}][y_{q,j} - \hat{y}_{j,q}] \rightarrow \min \quad (5)$$

where $\sigma_{i,j}$ corresponds to an element in the inverse of the error variance−covariance matrix, $y_{j,q}$ is the observed value for the physisorbed mole fraction of component i in experiment q and $\hat{y}_{j,q}$ is the corresponding model calculated value. The mole fractions are calculated according to eq 4. The separation factors at dense bulk phase conditions follow from the model developed in the physisorption section; see eqs 14 and 19. When estimating parameters from kinetic rather than physisorption data, molar outlet flow rates were used as responses, vide sections Reactor Model and Single-Event Microkinetics. The outlet flow rates were calculated according to model equations described by eq 6. The ODRPACK-package version 2.01 was used for regression.[24]

Reactor Model. The flow rates of the alkanes i, $\hat{F}_i$, follow from the integration of the corresponding continuity equations[25]

$$\frac{d\hat{F}_i}{dW} = R_i \quad (6)$$

The expressions for the net production rates of the components i, R_i, are discussed in the following section. The set of ordinary differential equations (ODEs) was integrated using the LSODA subroutine available on NETLIB.[26] The flow rate of the feed alkane was obtained from the elemental carbon balance. Hydrogen flow rates along the bed axis were calculated from the elemental hydrogen balance.

Thermodynamic Activity. The standard state used throughout this work is the ideal gas state. As a result deviations from ideality are assessed through fugacity coefficients. These coefficients are calculated using in-house-developed codes based on standard methodologies such as the Peng−Robinson equation of state.[27] Hydrogen interaction effects in the liquid phase are considered according to Moyson et al.[28]

Single-Event Microkinetics. Modeling hydroconversion kinetics using the single-event concept and considering the ideal bifunctional mechanism to occur is well documented.[29−32] Physisorption precedes dehydrogenation and protonation. (De)hydrogenation reactions and (de)protonation are assumed to be quasi-equilibrated. The only rate-determining steps are the acid-catalyzed skeletal isomerization and cracking reactions of the carbenium ions, i.e., nonbranching alkyl shifts, protonated cyclopropane (PCP) branching reactions, and β-scissions. Each of the latter can be classified into four reaction families, viz., (s,s), (s,t), (t,s), and (t,t) depending upon the secondary (s) or tertiary (t) nature of the reactant and product carbenium ions. Within a given reaction family the rate coefficient is assumed to depend only on the symmetry contributions of the reactant and the transition state, i.e., in particular to be independent of the carbon number. The symmetry dependence can be filtered out from the rate coefficient leading to a unique single-event rate coefficient for a given reaction family. Recently, "free carbenium ion reaction" activation energies and protonation enthalpies for hydroconversion reactions were reported based on vapor phase hydroconversion kinetics of alkanes.[33] The following expression for carbenium ion reactions was derived by linking the carbenium ion concentrations to the gas phase reactant partial pressures

$$r_k = \frac{C_t \frac{\sigma_j}{\sigma_\#} \tilde{k}(m_k;n)\tilde{K}_{prot}(m_k)K_{deh}C_{sat,i}K_{Lan,i}\frac{p_i}{p_{H_2}}}{1 + \sum_{j=1}^{n_{par}} K_{Lan,j}p_j + \sum_{j=1}^{n_{par}}\sum_{k=1}^{n_{car}} \frac{C_t\tilde{K}_{prot}(m_k)K_{deh}K_{Lan,j}\frac{p_j}{p_{H_2}}}{1 + \sum_{j=1}^{n_{par}}\sum_{k=1}^{n_{car}} \tilde{K}_{prot}(m_k)K_{deh}K_{Lan,j}\frac{p_j}{p_{H_2}}C_e}} \quad (7)$$

where C_t and $C_{sat,i}$ are the total concentration of Brönsted acid sites and the physisorption saturation concentration of alkane i. $\sigma_j/\sigma_\#$ is the ratio of the global symmetry numbers of the alkene j stemming from alkane i and the transition state, the so-called number of single events. K_{deh} is the (de)hydrogenation equilibrium coefficient, and $\tilde{k}(m_k,n)$ is the single-event rate coefficient for the conversion of a carbenium ion k of type m to type n. $\tilde{K}_{prot}(m_k)$ is the single-event (de)protonation equilibrium coefficient and $K_{Lan,i}$ is the Langmuir physisorption equilibrium coefficient for alkane i. A detailed description of the model and the corresponding parameter estimates can be found in the work of Thybaut et al.[33]

Note that the average acid strength of the catalyst is accounted for through the protonation equilibrium coefficient and more in particular through the standard protonation enthalpy of a reference alkene at an acid site.[31] Higher acid strengths correspond to higher values of the protonation coefficient and more negative values of the standard protonation enthalpy and, hence, to higher carbenium ion concentrations and reaction rates. Observations on catalysts with a different average acid site strength can be compared by accounting for these differences. Of course the differences in total acid site concentration should also be accounted for. The gas phase standard physisorption properties were obtained from Denayer et al.[10] The preexponential factors and activation energies were held at values reported elsewhere.[33] Similarly, the difference between the standard protonation enthalpies to secondary and tertiary carbenium ions was fixed at 35 kJ mol^{-1}.[33]

Physisorption of Hydrocarbons in Zeolites from a Dense Bulk Phase

Phenomenological Description. Excess Free Enthalpy for Physisorption. Typically, hydrocarbon physisorption properties are determined from vapor phase experiments.[10] These properties at ideal gas phase conditions are used in this work as reference to describe the physisorption from a more dense phase. Physisorption from a dense phase, e.g., a liquid, can be related to gas phase physisorption through a Born−Haber cycle; see Figure 3a.[15] The four corners in this Born−Haber cycle correspond to ideal vapor phase, dense bulk or liquid bulk phase,

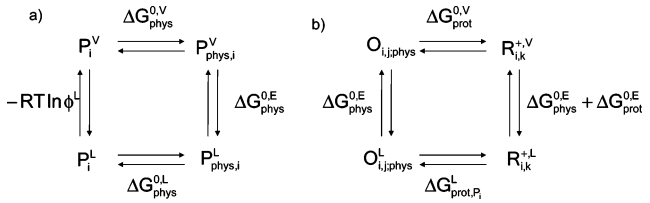

Figure 3. Born−Haber cycle for (a) vapor and liquid phase alkane physisorption and (b) vapor and liquid phase alkene protonation.

zeolite in contact with ideal vapor, and zeolite in contact with dense bulk or liquid bulk phase; see Figure 4

$$\Delta G^{0,\mathrm{L}}_{\mathrm{phys}} = -RT \ln \phi^{\mathrm{L}} + \Delta G^{0,\mathrm{V}}_{\mathrm{phys}} + \Delta G^{0,\mathrm{E}}_{\mathrm{phys}} \qquad (8)$$

where $\Delta G^{0,\mathrm{V}}_{\mathrm{phys}}$ is the standard free enthalpy of physisorption determined from ideal gas phase physisorption. The $RT \ln \phi^{\mathrm{L}}$ term accounts for the thermodynamic nonideality of the bulk phase with respect to the ideal gas state with ϕ the dense phase fugacity coefficient. $\Delta G^{0,\mathrm{E}}_{\mathrm{phys}}$ is the excess free enthalpy for physisorption and is discussed in the following paragraph.

Introducing the Langmuir physisorption equilibrium coefficient, eq 8 can be rewritten as

$$\Delta G^{0,\mathrm{L}}_{\mathrm{phys}} = -RT \ln \phi^{\mathrm{L}} - RT \ln K^{\mathrm{V}}_{\mathrm{Lan}} + \Delta G^{0,\mathrm{E}}_{\mathrm{phys}} \qquad (9)$$

Under the assumption that the bulk phase density has no impact on the physisorbed state, the thermodynamic activity of the physisorbed phase in equilibrium with the ideal gas phase is the same as that of the physisorbed phase in contact with the dense phase, for the same number of physisorbed sorbate molecules. Under this assumption, $\Delta G^{0,\mathrm{E}}_{\mathrm{phys}}$, the excess free enthalpy for physisorption in the dense phase compared to the ideal gas phase vanishes; i.e., $P^{\mathrm{V}}_{\mathrm{phys},i}$ becomes equal to $P^{\mathrm{L}}_{\mathrm{phys},i}$ in the Born−Haber cycle in Figure 3a, and the bulk phase density effect on the physisorption is exclusively attributed to "bulk phase nonideality"

$$\Delta G^{0,\mathrm{L}}_{\mathrm{phys}}\ (\text{bulk phase nonideality}) = -RT \ln \phi^{\mathrm{L}} + \Delta G^{0,\mathrm{V}}_{\mathrm{phys}} \qquad (10)$$

As it will be evident from the comparison between model calculations and experimental data, merely accounting for the bulk phase nonideality does not suffice to describe physisorption from a dense phase rather than an ideal gas phase. Hence, relaxing the assumption that the bulk phase density has no impact on the physisorbed state, the standard liquid phase physisorption free enthalpy can be written as

$$\Delta G^{0,\mathrm{E}}_{\mathrm{phys}} = \Delta G^{0,\mathrm{L}}_{\mathrm{phys}}\ (\text{bulk phase nonideality}) + \Delta G^{0,\mathrm{E}}_{\mathrm{phys}} \qquad (11)$$

The term excess is drawn from the analogy to liquid phase thermodynamic nonideality. $\Delta G^{0,\mathrm{E}}_{\mathrm{phys}}$ varies with the bulk phase density and becomes significant for dense bulk phases.[19−22] The intermolecular distances in a dense bulk phase are of molecular order, and entry or exit of a molecule from the dense bulk phase to the sorbent is felt by the neighboring molecules both in the dense bulk phase and in the entire physisorbed phase; see Figure 5. This can be looked at as a "compression" of the sorbate molecules. Repulsive interactions between these sorbate molecules become more important and destabilize the physisorbed state.[20,21] Because of the analogy of this effect to the bulk phase nonideality, which is expressed by the quantity $-RT \ln \phi^{\mathrm{L}}$, a proportionality between the standard excess free enthalpy for

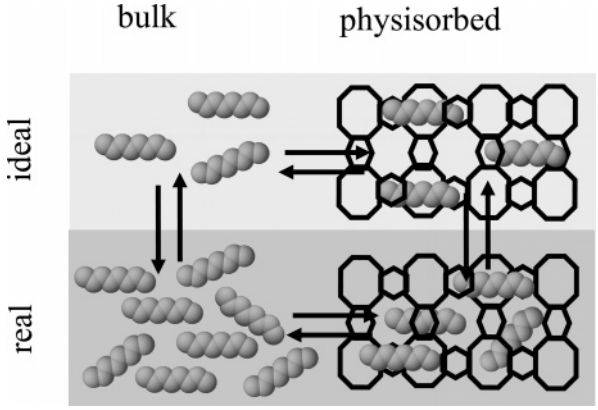

Figure 4. Schematic representation of the Born−Haber cycle for vapor and liquid phase alkane physisorption.

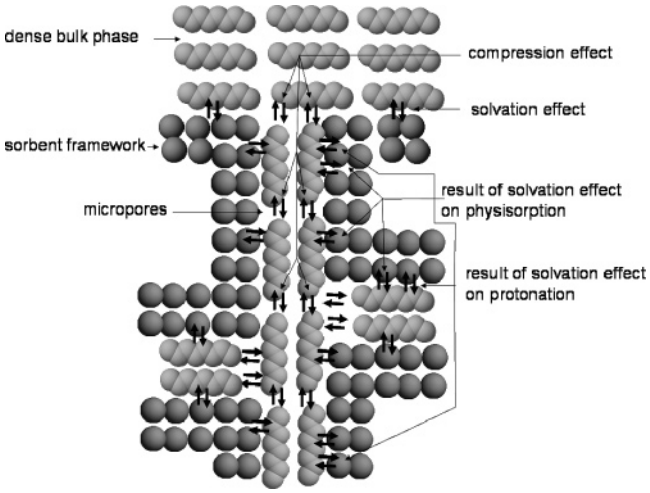

Figure 5. Schematic representation of our interpretation of the origin of the excess effects in physisorption in microporous sorbents.

physisorption and the logarithm of the fugacity coefficient for the species involved is put forward

$$\Delta G^{0,\mathrm{E}}_{\mathrm{phys}} = -c^{\mathrm{E}} \ln \phi^{\mathrm{L}} \qquad (12)$$

The corresponding proportionality factor, c^{E}, can be determined from physisorption data. Next to the so-called *compression*, the effet of bulk density may also be related to changes of the sorbent itself, see Figure 5**,** which can be interpreted as a "*solvation*" of the sorbent by the bulk phase. With a varying bulk phase density, the sorbent framework adapts its structure to establish the minimum free enthalpy configuration. As a result pore geometries can undergo small changes induced by variations in the bulk phase density. Because zeolite pore sizes are of molecular order, small changes in pore size can have important effects on the physisorption properties.

Madon and Iglesia[8] have developed a comprehensive treatment of zeolite catalysis in which they consider the species in the zeolite pores as being solvated. In our terminology, the solvation as described by Madon and Iglesia[8] depends on the density of the bulk phase in which the zeolite is contained.

The excess free enthalpy for physisorption as it has been put forward above encompasses but goes beyond binary sorbate sorbate interactions. The effect of binary sorbate sorbate interactions has been assessed by Denayer et al.[34] at pore filling conditions and was found to lead to a decrease in separation factors between the hydrocarbons involved. At high bulk phase density conditions, however, a further reduction of the separation

CHART 1. Phenomena Involved in Physisorption and the Corresponding Terms in Physisorption Modeling

physisorption from ideal gas	physisorption from dense bulk phase	corresponding term
	bulk phase non ideality	$-RT\ln\phi^{L}$
physisorption step	physisorption step	$\Delta G^{0,V}_{phys}$
	physisorption excess (compression and solvation)	$\Delta G^{0,E}_{phys} = -c^{E}\ln\phi^{L}$

factors is observed[23] justifying the more comprehensive methodology presented in this work to describe physisorption at dense phase conditions.

The phenomena involved in physisorption are summarized in Chart 1. Physisorption is a stabilizing process leading to surface enrichment of the sorptive molecules. This corresponds to the term $\Delta G^{0,V}_{phys}$. When physisorption occurs from a dense phase rather than an ideal vapor phase, two additional, destabilizing, contributions are invoked to describe this physisorption, i.e., the bulk phase nonideality, $-RT\ln\phi^{L}$, and the excess free enthalpy for physisorption, $\Delta G^{0,E}_{phys} = -c^{E}\ln\phi^{L}$. The excess free enthalpy for physisorption is proposed as the result of a direct compression of the adsorbates in the catalyst pores by the dense bulk phase. The extent of the compression can be affected by a solvation of the catalyst framework. The extent of destabilization depends on the density of the bulk fluid and of the sorbent force field acting on the sorbate molecules. The stronger the force field, the higher are both stabilization and destabilization effects. For an ideal gas phase the physisorption destabilization does not prevail whether the sorbent is strongly or weakly interacting with the sorbate molecules.[20,21] The terms $-RT\ln\phi^{L}$ and $\Delta G^{0,E}_{phys}$ become important only with increasing density of the bulk phase, e.g., liquid phase or high-pressure nonideal gas phase.

Values for the newly introduced parameter c^{E} can be obtained by regression of binary liquid phase physisorption isotherms for a given zeolite. Equation 9 can now be rewritten as

$$\Delta G^{0,L}_{phys} = -RT\ln K^{V}_{Lan} - (RT + c^{E})\ln\phi^{L} \qquad (13a)$$

or, in terms of equilibrium coefficients, as

$$K^{L}_{Lan} = K^{V}_{Lan}(\phi^{L})^{(1+(c^{E}/RT))} = K^{V}_{Lan}K^{E}_{phys}(\phi^{L}) \qquad (13b)$$

where

$$K^{E}_{phys} = (\phi^{L})^{(c^{E}/RT)} = \exp\left(\frac{-\Delta G^{0,E}_{phys}}{RT}\right) \qquad (14)$$

Finally, note here that $\Delta G^{0,E}_{phys}$ is a single-component property determined from liquid phase physisorption experiments.

Generalized Langmuir Isotherm for Physisorption. Different methodologies to model liquid phase physisorption have been developed[14] and are based on either Langmuir models or ideal and real adsorption solution theories.[12,35,36] Langmuir models are reported to be widely applied with success, and hence, they are used in the present work.[14,20,21] Langmuir models are especially practical for use in multicomponent reaction modeling. These models are easier to implement than, e.g., ideal or real adsorption solution theory. It should be kept in mind, however, that the molar volumes of the mixture compounds should not be too different when describing multicomponent physisorption using a Langmuir model.

Generalization of the vapor phase Langmuir isotherm to any fluid phase for a component i is carried out via fugacities referring to the ideal gas state as standard state

$$C_{phys,i} = \frac{K^{V}_{Lan,i}K^{E}_{phys,i}C_{sat,i}f_i}{1 + \sum_j K^{V}_{Lan,j}K^{E}_{phys,j}f_j} \qquad (15)$$

The fugacity coefficients ϕ_i are incorporated into the fugacities f_i. For the case of vapor phase physisorption, the fugacity f^{V}_i is written as the product of the fugacity coefficient and the partial pressure

$$f^{V}_i = \phi^{V}_i p_i \qquad (16)$$

If the vapor phase phase can be considered as an ideal gas, the fugacity coefficient equals 1 and, hence, the fugacity from eq 15 reduces to the partial pressure. For hydrocarbons this assumption is valid at sufficiently low pressures. However, at high pressures deviations from the ideal gas state have to be considered.

For the case of liquid phase physisorption, the fugacities are expressed in terms of the concentration of a species i in the liquid phase, C^{L}_i, its fugacity coefficient ϕ^{L}_i, the total pressure p_i, and the molar volume of the liquid, V_m

$$f^{L}_i = \phi^{L}_i\ C^{L}_i\ V_m\ p_t \qquad (17)$$

As a result, starting from eq 15 and introducing the expression for the excess physisorption coefficient, eq 14, the physisorbed concentration of a component i from a liquid phase can be expressed as follows

$$C_{phys,i} = \frac{K^{V}_{Lan,i}(\phi^{L}_i)^{(1+(c^{E}/RT))}p_tV_mC^{L}_i}{1 + \sum_j K^{V}_{Lan,j}(\phi^{L}_j)^{(1+(c^{E}/RT))}p_tV_mC^{L}_j} \qquad (18)$$

Comparison between Model Calculations and Experimental Data. With eq 18, first a description of binary isotherms is attempted to assess the effect of dense bulk phase on the separation factor. From eqs 1 and 18 the following expression for the separation factor can be obtained

$$\alpha_{i-j} = \frac{K^{V}_{Lan,i}C_{sat,i}\phi_i K^{E}_{phys,i}}{K^{V}_{Lan,j}C_{sat,j}\phi_j K^{E}_{phys,j}} = \frac{H_i\phi_i K^{E}_{phys,i}}{H_j\phi_j K^{E}_{phys,j}} \qquad (19)$$

For an ideal gas, the fugacity coefficient and the excess physisorption equilibrium coefficient are equal to 1 and, hence, the vapor phase separation factors correspond to the ratio of the measured Henry coefficients

$$\alpha_{i-j} = \frac{K^{V}_{Lan,i}C_{sat,i}}{K^{V}_{Lan,j}C_{sat,j}} = \frac{H_i}{H_j} \qquad (20)$$

As shown in Figure 1, eq 20 allows adequate description of the vapor phase separation factors. Comparison of this ratio of Henry coefficients to the liquid phase separation factors allows assessment of the effect of the fluid phase bulk density on the adsorption behavior.

Equation 19 also applies for the calculation of separation factors for liquid phase physisorption. For this purpose, apart from the Henry coefficient, two additional values are required: (i) the liquid phase fugacity coefficient, ϕ^{L}_i, accounting for the deviation of the bulk fluid from ideal gas state and (ii) the excess free enthalpy parameter, c^{E}, accounting for the effect of bulk fluid phase density on the physisorbed state.

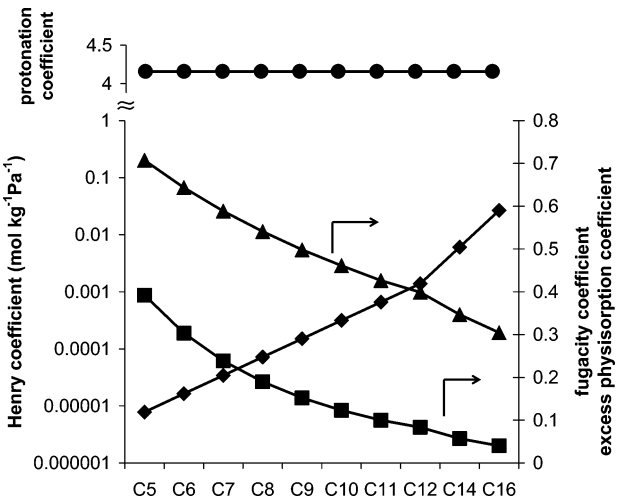

Figure 6. Henry coefficient, ◆, fugacity coefficient, ■, excess physisorption coefficient K^{E}_{phys}, ▲, and excess protonation coefficient K^{E}_{prot}, ●, calculated at $T = 506$ K, $p_t = 8.0$ MPa. Henry coefficients are obtained from measured standard physisorption properties for USY (CBV-760).[23,10] Fugacity coefficients calculated from the Peng−Robinson equation of state.[37] Excess physisorption coefficient is calculated from eq 14 with c^E equal to 1.55 kJ mol^{-1}.

At ambient conditions, the values for the calculated fugacity coefficients decrease strongly with the carbon number and vary from 0.3 for C_5 to 10^{-7} for C_{16}. At the experimental hydroconversion conditions of 506 K and 8.0 MPa, the values of fugacity coefficients for C_5 to C_{16} range from 0.4 to 0.04; see Figure 6.

Only accounting for the bulk phase non ideality, i.e., assuming the excess physisorption coefficient, $K^{E}_{phys,i}$, equal to 1, the separation factors are calculated from

$$\alpha^{L}_{i-j}(\text{bulk phase nonideality}) = \frac{H_i\,\phi_i}{H_j\,\phi_j} \qquad (21)$$

The fugacity coefficients are lower than 1, and hence, the physisorption stabilization when accounting for bulk phase nonideality is less pronounced compared to the physisorption stabilization at ideal vapor phase conditions; i.e., for ϕ_i, see eq 18. The higher the carbon number, the lower the fugacity coefficient and, hence, the physisorption stabilization decreases with the carbon number. As a result, the carbon number dependence of the separation factors α^{L}_{i-j}(bulk phase nonideality) decreases compared to the that of the ratio of Henry coefficients, α^{L}_{i-j}; see Figure 1.

A non-negligible discrepancy can be observed between the liquid phase separation factors, which are essentially equal to 1, and the separation factors calculated only accounting for bulk phase nonideality; see Figure 1**.** When accounting for the excess free enthalpy of physisorption at dense phase conditions, the carbon number dependency of the separation factors is becoming even less pronounced. This is in agreement with the results from molecular simulations[37] and other theoretical work.[38] The magnitude of this effect was not calculated a priori but has been estimated through the excess free enthalpy parameter c^E via regression.

c^E was estimated at 1.55 ± 0.04 kJ mol^{-1} with F values for the significance of the regression above 8000. The positive value for c^E indicates that excess free enthalpy for physisorption, see eq 12, destabilizes the adsorbate molecules due to repulsive interactions in the physisorbed phase as explained above. The separation factors calculated using the estimated value for c^E are in reasonable agreement with the experimentally obtained separation factors; see Figure 1. Accounting for the excess free enthalpy in physisorption through the fluid phase fugacity coefficient allows adequate description of the effect of bulk fluid density on physisorption. Having adequately described physisorption in liquid phase, the description of liquid phase kinetics is now attempted.

Liquid Phase Hydroconversion

Effect of Bulk Fluid Phase Density on Protonation. The bulk phase density affects the physisorbed state and, hence, may also affect the elementary steps in which the physisorbed species are involved. In particular, the elementary step in which the physisorbed species interacts with the sorbent framework, i.e., the protonation, is considered. A Born−Haber cycle linking protonation in the presence of bulk vapor phase to protonation in the presence of bulk liquid phase is shown in Figure 3b. The liquid phase standard free enthalpy for protonation is linked to vapor phase standard free enthalpy for protonation by the following relationship, analogous to eq 11

$$\Delta G^{0,L}_{prot} = \Delta G^{0,L}_{prot}(\text{bulk phase nonideality}) + \Delta G^{0,E}_{prot} \qquad (22)$$

where $\Delta G^{0,E}_{prot}$ is the standard excess protonation free enthalpy, which pertains to changes in interaction between the ionic center of the carbenium ion and the deprotonated acid site in the zeolite in a dense bulk phase compared to in an ideal gas phase. Because only the ionic center is involved, no dependence of the excess protonation free enthalpy on the carbon number is assumed. In agreement with earlier work,[31] enthalpic rather than entropic effects are considered.

The excess standard protonation enthalpy is estimated from liquid phase kinetic data on CBV-720. The rate equation for an elementary step consuming carbenium ion k stemming from alkane i in liquid phase is expressed as follows

$$r_k = \left\{ C_t \frac{\sigma_j}{\sigma_\#} \tilde{k}(m_k;n) \tilde{K}^{E}_{prot} \tilde{K}_{prot}(m_k) K_{deh} C_{sat,i} K_{Lan,i} \phi^{L}_i K^{E}_{phys,i} \frac{C_i}{C_{H_2}\phi^{L}_{H_2}} \right\} \Big/ \left\{ 1 + \sum_{j=1}^{n_{par}} K_{Lan,j} \phi^{L}_j K^{E}_{phys,j} V_m C_j p_t + \sum_{j=1}^{n_{par}} \sum_{k=1}^{n_{car}} \times \right.$$

$$\left. \frac{C_t \tilde{K}^{E}_{prot} \tilde{K}_{prot}(m_k) K_{deh} K_{Lan,j} \phi^{L}_j K^{E}_{phys,j} \dfrac{C_j}{C_{H_2}\phi^{L}_{H_2}}}{1 + \sum_{j=1}^{n_{par}} \sum_{k=1}^{n_{car}} \tilde{K}^{E}_{prot} \tilde{K}_{prot}(m_k) K_{deh} K_{Lan,j} \phi^{L}_j K^{E}_{phys,j} \dfrac{C_j}{C_{H_2}\phi^{L}_{H_2}} C_e} \right\} \qquad (23)$$

The above equation is identical to eq 7 except for the additional terms $K^{E}_{phys,j}$, $\tilde{K}^{E}_{prot}$, and ϕ^{L}_i accounting for differences between vapor and liquid phase. Regression with the liquid phase model, eq 23, of earlier reported data for liquid phase hydroconversion of a nC_7-nC_9 mixture[2] with only the excess standard protonation enthalpy, $\Delta H^{0,E}_{prot}$, as adjustable parameter led to an estimated value of −7.8 ± 1.0 kJ mol^{-1}. The corresponding value for the liquid phase standard protonation

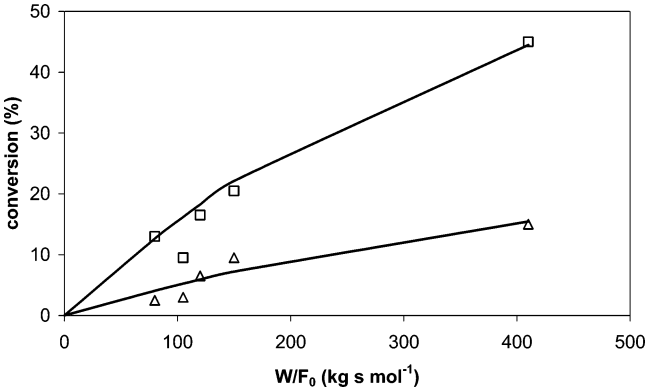

Figure 7. Conversion versus W/F_0 for liquid phase n-C_7:n-C_9 hydroconversion at 503 K and 10 MPa: symbols, experimental n-C7 (△) and n-C9 (□) conversion;[1,2] full lines, SEMK model calculations using eq 23. Activation energies, protonation enthalpies, and values for the preexponential factors are as in ref 33; the excess standard protonation enthalpy amounted to -7.8 kJ mol^{-1}.

enthalpy for secondary carbenium ion formation, $\Delta H_{\text{prot}}^{0,\text{L}}$, is -74.2 kJ mol^{-1}. The conversion versus space time behavior is well described by the model for both heptane and nonane; see Figure 7.

Vapor versus Liquid Phase Activity. At liquid phase conditions physisorption will occur in the saturation regime. At vapor phase conditions, the physisorption regime strongly depends on the hydrocarbon partial pressures and on the carbon number. For lighter hydrocarbons and lower partial pressures, physisorption will occur in the Henry regime, while for heavier hydrocarbons and higher partial pressures physisorption saturation will rather occur. As a result, the two limiting cases at vapor phase conditions will be considered. Throughout this discussion, carbenium ion concentrations are assumed to be small.[33] The mathematical corollary of this assumption is that the last term in the denominator of eqs 7 and 23 can be neglected.

Upon physisorption saturation the liquid phase hydroconversion rate can be approximated as

$$r_k^{\text{L}} = C_{\text{t}} \frac{\sigma_j}{\sigma_\#} \tilde{k}(m_k;n)\, \tilde{K}_{\text{prot}}^{\text{E}}\, \tilde{K}_{\text{prot}}(m_k) K_{\text{deh}} C_{\text{sat},i} \frac{1}{V_m p_{\text{t}} C_{\text{H}_2} \phi_{\text{H}_2}^{\text{L}}} \quad (24)$$

whereas the vapor phase hydroconversion rate in the Henry regime can be written as

$$r_k^{\text{V}} = C_{\text{t}} \frac{\sigma_j}{\sigma_\#} \tilde{k}(m_k;n) \tilde{K}_{\text{prot}}(m_k) K_{\text{deh}} C_{\text{sat},i} K_{\text{Lan},i} \frac{p_i}{p_{\text{H}_2}} \quad (25)$$

The ratio of these two rates leads to

$$\frac{\tilde{K}_{\text{prot}}^{\text{E}}}{K_{\text{Lan},i}\, p_i\, \phi_{\text{H}_2}^{\text{L}}} \quad (26)$$

Given the values for the terms in this ratio, $\tilde{K}_{\text{prot}}^{\text{E}} \approx 4$, $\phi_{\text{H}_2}^{\text{L}} \approx 10$, and $K_{\text{Lan},i} p_i < 10^{-1}$, liquid phase conditions are enhancing the hydroconversion rates if the physisorption at vapor phase conditions falls within the Henry regime. If on the other hand physisorption saturation occurs at vapor phase conditions, the vapor phase hydroconversion rate is expressed as follows

$$r_k^{\text{V}} = C_{\text{t}} \frac{\sigma_j}{\sigma_\#} \tilde{k}(m_k;n) \tilde{K}_{\text{prot}}(m_k) K_{\text{deh}} C_{\text{sat},i} \frac{1}{p_{\text{H}_2}} \quad (27)$$

TABLE 1: Competition Factor $\varsigma_{C_9-C_7} = r_{0,C_9}/r_{0,C_7}$ for Pt/H−USY (CBV-720) for Vapor and Liquid Phase Hydroconversion of a n-C_7 n-C_9 Mixture: Comparison between Experimental[1,2] and Calculated Values from the Vapor, Eq 7, and Liquid, Eq 23, Phase Single-Event Microkinetic Model[a]

	experimental	model
vapor phase	8.4	9.5
liquid phase	2.7	4.0

[a] Activation energies, protonation enthalpies, and values for the preexponential factors are as in ref 33; the excess protonation enthalpy amounted to -7.8 kJ mol^{-1}.

and the ratio of the hydroconversion rates between liquid and vapor phase is given by

$$\frac{\tilde{K}_{\text{prot}}^{\text{E}}}{\phi_{\text{H}_2}^{\text{L}}} \quad (28)$$

and only a moderate effect of the aggregation state on the total conversion is expected.

Vapor versus Liquid Phase Selectivity. A significant reduction of the "competition factor", defined as the ratio of the initial conversion rates of n-nonane and n-heptane in mixtures, $\varsigma_{C_9-C_7} = r_{0,C_9}/r_{0,C_7}$, is observed when going from vapor- to liquid phase conditions.[1,2] At vapor phase conditions, this competition factor corresponds to the ratio of the product of the composite rate coefficient, the Henry coefficient, and the hydrocarbon partial pressure

$$\varsigma_{C_9-C_7}^{\text{V}} = \frac{k_{C_9}^{\text{comp}} H_{C_9} p_{C_9}}{k_{C_7}^{\text{comp}} H_{C_7} p_{C_7}} = \alpha_{C_9-C_7}^{\text{V}} \frac{k_{C_9}^{\text{comp}} p_{C_9}}{k_{C_7}^{\text{comp}} p_{C_7}} \quad (29)$$

in which

$$k_i^{\text{comp}} = k_i K_{\text{prot}} K_{\text{deh},i} \quad (30)$$

At liquid phase conditions the fugacity coefficients and the excess coefficients for physisorption have also to be accounted for

$$\varsigma_{C_9-C_7}^{\text{L}} = \frac{k_{C_9}^{\text{comp}} H_{C_9} K_{\text{phys},C_9}^{\text{E}} \phi_{C_9}^{\text{L}} p_{C_9}}{k_{C_7}^{\text{comp}} H_{C_7} K_{\text{phys},C_7}^{\text{E}} \phi_{C_7}^{\text{L}} p_{C_7}} = \alpha_{C_9-C_7}^{\text{L}} \frac{k_{C_9}^{\text{comp}} p_{C_9}}{k_{C_7}^{\text{comp}} p_{C_7}} \quad (31)$$

with

$$k_i^{\text{comp}} = k_i K_{\text{prot}} K_{\text{prot}}^{\text{E}} K_{\text{deh},i} \quad (32)$$

Table 1 shows a comparison of the competition factors calculated using eqs 29 and 31 with the experimental values reported by Denayer et al.[2] A reasonable agreement is observed for both aggregation states. The competition factor is between two and three times lower in the liquid phase. This is due to the liquid phase fugacity coefficient, ϕ_i^{L}, and the excess coefficient for physisorption, $K_{\text{phys},i}^{\text{E}}$, which are incorporated in the separation factor; see eq 19. The ratio $K_{\text{phys},C_9}^{\text{E}} \phi_{C_9}^{\text{L}} / K_{\text{phys},C_7}^{\text{E}} \phi_{C_7}^{\text{L}}$ amounts to 0.4, which explains the 2.5-fold decrease of the competition factor at liquid phase conditions; see Table 1. It is evident from eqs 29 to 32 that the separation factor is affected to the same extent.

As for physisorption, the differences in selectivity between vapor- and liquid phase hydroconversion are of a thermodynamic nature. The bulk fluid density affects the thermodynamic

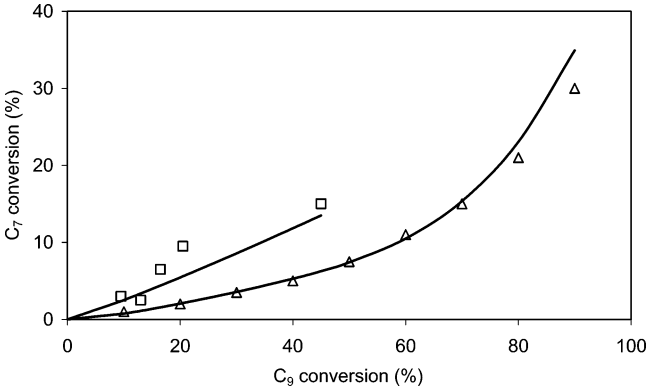

Figure 8. *n*-C_9 versus *n*-C_7 conversion in vapor and liquid phase hydroconversion of an equimolar *n*-C_7:*n*-C_9 mixture. Symbols: △, vapor phase data; □, liquid phase data;[1,2] full lines, SEMK model calculations using eq 7 at vapor phase conditions and eq 23 at liquid phase conditions. Activation energies, protonation enthalpies, and values for the preexponential factors are as in ref 33; the excess standard protonation enthalpy amounted to −7.8 kJ mol^{-1}.

activity of the components in the fluid and in the physisorbed phase and, hence, the kinetics. The liquid phase fugacity coefficient of *n*-C_9 is significantly lower than that of *n*-C_7, see Figure 6, which lowers the hydroconversion rate of *n*-C_9 relative to that of *n*-C_7 at liquid phase conditions. As a result, the preferential *n*-C_9 conversion at vapor phase conditions is less pronounced at liquid phase conditions. This effect has also been denoted as an "enhanced competition" of *n*-C_7 with *n*-C_9 at liquid phase conditions.[2] On top of the bulk phase nonideality, the excess free enthalpy for physisorption, ΔG^{E}_{phys}, is further enhancing the *n*-C_7 conversion compared to the *n*-C_9 conversion. Figure 8 shows a comparison between observed and calculated competition effects at vapor and liquid phase conditions.

The expression for the competition factor at liquid phase conditions, eq 31, can be simplified into

$$\varsigma^{L}_{C_9-C_7} \overset{USY}{=} \frac{K^{comp}_{C_9} p_{C_9}}{K^{comp}_{C_7} p_{C_7}} \tag{33}$$

because the carbon number effect on the fugacity coefficient and the excess physisorption coefficient is almost perfectly compensating for the carbon number effect on the Henry coefficient and, hence, leads to separation factors close to 1. Competition in hydroconversion of binary mixtures is governed by the chemical reactivity of the components, i.e., the composite rate coefficients, and by their physical interactions with the catalyst framework, i.e., the Henry coefficients; see eq 29 at vapor phase conditions. At liquid phase conditions only differences in chemical reactivity, i.e., the composite rate coefficients, remain; see eq 33. The higher chemical reactivity of *n*-nonane originates from its more extended reaction network.

Conclusions

To describe liquid phase hydroconversion kinetics on Pt/H−USY-zeolites, it is necessary and sufficient to account for the bulk phase thermodynamic nonideality as well as physisorption destabilization and protonation stabilization. The latter effects can be interpreted in terms of a compression effect of the dense fluid phase on the sorbate molecules and a solvation effect on the sorbent framework.

For a given catalyst only two parameters, i.e., the excess physisorption coefficient and the excess standard protonation enthalpy have to be estimated from experimental data to apply a single-event microkinetic model based on vapor phase data to liquid phase conditions. The former coefficient describes the physisorption destabilization, while the latter accounts for the modified protonation behavior. A negative excess standard protonation enthalpy is obtained at dense phase conditions. This enhances the reaction rates and compensates for the physisorption excess which lowers the physisorbed concentrations. The net effect of excess physisorption and protonation is moderate. Liquid phase hydroconversion rates are of the same order of magnitude as vapor phase hydroconversion rates. Selectivities in binary mixture hydroconversion strongly depend on the aggregation state. Lighter hydrocarbons are more competitive at liquid phase conditions than at vapor phase conditions.

Glossary

C	concentration (mol kg_{cat}^{-1})
c^E	excess free enthalpy parameter for physisorption (kJ mol^{-1})
F	molar flow rate (mol s^{-1})
f	fugacity (Pa)
G	free enthalpy (kJ mol^{-1})
H	Henry coefficient (mol kg_{cat}^{-1} Pa^{-1})
H	enthalpy (kJ mol^{-1})
i	component index
j	component index
K	equilibrium coefficient
K_{Lan}	Langmuir physisorption coefficient (Pa^{-1})
$k(m,n)$	rate coefficient of a reaction converting a carbenium ion of type m into another carbenium ion of type n (s^{-1})
m	carbenium ion type (secondary or tertiary)
n	carbenium ion type (secondary or tertiary)
n	number
p	(partial) pressure (Pa)
q	experiment index
R	net production rate (mol (kg_{cat} s)$^{-1}$)
R	universial gas constant (8.31451 J (mol K)$^{-1}$)
r	reaction rate of an elementary step (mol (kg_{cat} s)$^{-1}$)
$S(b)$	objective function
s	secondary carbenium ion
t	tertiary carbenium ion
T	temperature (K)
V_m	molar volume (m^3 mol^{-1})
W	catalyst weight (kg)
x	mole fraction in the bulk phase
y	mole fraction in the physisorbed phase

Greek Symbols

α_{i-j}	separation factor in binary mixture with components i and j[10,23]
Δ	difference
ϕ	fugacity coefficient
ς_{i-j}	competition factor, i.e., ratio of initial rates for components i and j in the reaction mixture
σ	global symmetry number
$\sigma_{i,j}$	element of the ith row and jth column of the inverse error covariance matrix

Superscripts

o	standard state
∼	single event
∧	model calculated value
comp	composite
E	excess

exp	experimental
L	liquid
V	vapor

Subscript

0	inlet
#	transition state
car	carbenium ion
deh	dehydrogenation
e	empty
i	component *i*
j	component *j*
k	component (carbenium ion) *k*
ob	observation
ole	alkenes
par	alkanes
phys	physisorption
prot	protonation
q	observation *q*
resp	response
sat	saturation
t	total

Acknowledgment. This research was carried out in the framework of Interuniversity Attraction Poles Programme funded by the Belgian Science Policy.

References and Notes

(1) Denayer, J. F. M.; De Jonckheere, B. A.; Hloch, M.; Marin, G. B.; Vanbutsele, G.; Martens, J. A.; Baron, G. V. *J. Catal.* **2002**, *210*, 445.

(2) Denayer, J. F. M.; Ocakoglu, A. R.; De Jonckheere, B. A.; Martens, J. A.; Thybaut, J. W.; Marin, G. B.; Baron, G. V. *Int. J. Chem. React. Eng.* **2003**, *1*, A36.

(3) Arroyo J. A. M.; Martens G. G.; Froment G. F.; Marin G. B.; Jacobs P. A.; Martens J. A. *Appl. Catal., A* **2000**, *192*, 9.

(4) Amis, E. S. *Solvent effects on reaction rates and mechanisms*; Academic Press: New York, 1966.

(5) Iglesia, E.; Reyes, C. S.; Madon, R. J. *J. Catal.* **1991**, *129*, 238.

(6) Iglesia, E. *Appl. Catal., A* **1997**, *161*, 59.

(7) Madon, R. J.; O'Connel, J. P.; Boudart, M. *AIChE J.* **1978**, *24*, 904.

(8) Madon, R. J.; Iglesia, E. *J. Mol. Catal., A*: *Chem.* **2000**, *163*, 189.

(9) Thybaut, J. W.; Saeys, M.; Marin, G. B. *Chem. Eng. J.* **2002**, *90*, 117.

(10) Denayer, J. F. M.; Baron, G. V. *Adsorption* **1997**, *3*, 1.

(11) Adamson, A. W. *Physical chemistry of surfaces*; John Wiley & Sons: New York, 1967.

(12) Myers, A. L. *AIChE J.* **2002**, *48*, 145.

(13) Do, D. D.; Do, H. D. *AIChE J.* **2002**, *48*, 2213.

(14) Al-Duri, B. *Rev. Chem. Eng.* **1995**, *11*, 101.

(15) Chempath, S.; Snurr, R. Q.; Low, J. J. *AIChE J.* **2004**, *50*, 463.

(16) Ustinov, E. A.; Do, D. D.; Herbst, A.; Staudt, R.; Harting, P. *J. Colloid Interface Sci.* **2002**, *250*, 49.

(17) Wood, B. D.; Quntard, M.; Whitaker, S. *Chem. Eng. Sci.* **2004**, *59*, 1905.

(18) Erickson, J. S.; Aranovich, G. L.; Donohue, M. D. *Mol. Phys.* **2002**, *100*, 2121.

(19) Hill, T. L. *Proc. Natl. Acad. Sci. U.S.A.* **1996**, *93*, 14328.

(20) Aranovich, G. L.; Donohue, M. D. *Colloids Surf., A* **2001**, *187*, 95.

(21) Aranovich, G. L.; Donohue, M. D. *Langmuir* **2003**, *19*, 2722.

(22) Wetzel, T. E.; Erickson, J. S.; Donohue, P. S.; Charniak, C. L.; Aranovich, G. L.; Donohue, M. D. *J. Chem. Phys.* **2004**, *120*, 11765.

(23) Denayer J. F.; Bouyermaouen A.; Baron G. V. *Ind. Eng. Chem. Res.* **1998**, *37*, 3691.

(24) Boggs, P. T.; Donaldson J. R.; Byrd R. H.; Schnabel R. B. *ACM Trans. Math. Soft.* **1989**, *15*, 348.

(25) Froment, G. F.; Bischoff, K. B. *Chemical Reactor Analysis and Design*, 2nd ed.; Wiley: New York, 1990.

(26) NETLIB, http://www.netlib.org

(27) Reid, R. C.; Prausnitz, J. M.; Poling, B. E. *The properties of gases and liquids*, 4th ed.; McGraw-Hill: Singapore, 1988.

(28) Moysan, M.; Huron, M. J.; Paradowsky, H.; Vidal, J. *Chem. Eng. Sci.* **1983**, *38*, 1085.

(29) Martens, G. G.; Marin, G. B.; Martens, J. A.; Jacobs, P. A.; Baron, G. V. *J. Catal.* **2000**, *195*, 253.

(30) Martens, G. G.; Thybaut, J. W.; Marin, G. B. *Ind. Eng. Chem. Res.* **2001**, *40*, 1832.

(31) Thybaut, J. W.; Marin, G. B.; Baron, G. V.; Jacobs, P. A.; Martens, J. A. *J. Catal.* **2001**, *202*, 324.

(32) Thybaut, J. W.; Marin, G. B. *Chem. Eng. Technol.* **2003**, *26*, 509.

(33) Thybaut, J. W.; Laxmi Narasimhan, C. S.; Marin,.G. B.; Denayer, J. F. M.; Baron, G. V.; Jacobs, P. A.; Martens, J. A. *Catal. Lett.* **2004**, *94*, 81.

(34) Denayer, J. F.; Baron, G. V.; Jacobs, P. A.; Martens, J. A. *Phys. Chem. Chem. Phys.* **2000**, *2*, 1007.

(35) Krishna, R.; Baur, R. *Sep. Purif. Technol.* **2003,** *33*, 213.

(36) Krishna, R. *Trans IchemE* **2001**, *79*, 182.

(37) Schenk, M.; Calero, S.; Maesen, T. L. M.; Van Benthem, L. L.; Verbeek, M. G.; Smit, B. *Angew. Chem., Int. Ed.* **2002**, *41*, 2499.

(38) Talbot, J. *AIChE J.* **1997**, *43*, 2471.